Published in final edited form as:
Proteins. 2012 May ; 80(5): 1436–1447. doi:10.1002/prot.24042.

Crystal structure and biochemical properties of putrescine carbamoyltransferase from *Enterococcus faecalis*: assembly, active site and allosteric regulation

Dashuang Shi[1,*], **Xiaolin Yu**[1], **Gengxiang Zhao**[1], **Jeremy Ho**[1], **Shennon Lu**[1], **Norma M. Allewell**[2], and **Mendel Tuchman**[1]

[1]Center for Genetic Medicine Research and Department of Integrative Systems Biology, Children's National Medical Center, The George Washington University, Washington, 111 Michigan Avenue, Washington, DC 20010, USA

[2]Department of Cell Biology and Molecular Genetics and Department of Chemistry and Biochemistry, College of Computer, Mathematical, and Natural Sciences, University of Maryland, College Park, MD 20742, USA

Abstract

Putrescine carbamoyltransferase (PTCase) catalyzes the conversion of carbamoylputrescine to putrescine and carbamoyl phosphate (CP), a substrate of carbamate kinase (CK). The crystal structure of PTCase has been determined and refined at 3.2 Å resolution. The trimeric molecular structure of PTCase is similar to other carbamoyltransferases, including the catalytic subunit of aspartate carbamoyltransferase (ATCase) and ornithine carbamoyltransferase (OTCase). However, in contrast to other trimeric carbamoyltransferases, PTCase binds both CP and putrescine with Hill coefficients at saturating concentrations of the other substrate of 1.53 ± 0.03 and 1.80 ± 0.06, respectively. PTCase also has a unique structural feature: a long *C*-terminal helix that interacts with the adjacent subunit to enhance intersubunit interactions in the molecular trimer. The *C*-terminal helix appears to be essential for both formation of the functional trimer and catalytic activity, since truncated PTCase without the *C*-terminal helix aggregates and has only 3% of native catalytic activity. The active sites of PTCase and OTCase are similar, with the exception of the 240's loop. efPTCase lacks the proline-rich sequence found in knotted carbamoyltransferases and is unknotted. A Blast search of all available genomes indicates that 35 bacteria, most of which are Gram-positive, have an *agcB* gene encoding PTCase located near the genes that encode agmatine deiminase and carbamate kinase, consistent with the catabolic role of PTCase in the agmatine degradation pathway. The *C*-terminal helix identified in efPTCase is found in all other PTCases identified, suggesting that it is the signature feature of the PTCase family of enzymes.

Keywords

agmatine degradation; arginine degradation; putrescine carbamoyltransferase; ornithine carbamoyltransferase; crystal structure

[*]To whom correspondence should be addressed: Center for Genetic Medicine Research and Department of Integrative Systems Biology Children's National Medical Center, The George Washington University 111 Michigan Avenue, N.W. Washington, D.C. 20010-2970 Telephone: (202)476-5817; Fax: (202)476-6014; dshi@cnmcresearch.org.

INTRODUCTION

The arginine and agmatine degradation pathways enable arginine and agmatine, respectively, to be used as energy sources by *Enterococcus faecalis* (formerly *Streptococcus faecalis*)[1]. These catabolic pathways involve the sequential actions of three enzymes: arginine deiminase (ADI, locus-tag EF0104), catabolic ornithine carbamoyltransferase (OTCase, EF0105), pathway-specific carbamate kinase (CK, EF0106) in the arginine degradation pathway; and agmatine deiminase (AgDI, EF0734), putrescine carbamoyltransferase (PTCase, EF0732), and pathway-specific CK (EF0735) in the agmatine degradation pathway[2,3]. Analogous enzymes in the two pathways have significant sequence similarity.

PTCase was first identified forty years ago when it was found that Gram-positive *Streptococcus* (now *Enterococcus*) was able to grow on agmatine as the primary energy source[3]. Further studies indicated that PTCase efficiently catalyzed the carbamoylation of putrescine and had weak but unambiguous OTCase activity[4]. The first 29 *N*-terminal amino acids of purified PTCase were determined by Tricot (1989)[5]. The complete genome of *E. faecalis* has now been sequenced[6] and four carbamoyltransferase-like genes (EF0732, EF0105, EF2517 and EF1719) have been identified. One was annotated as the *pyrB* gene (EF1719) that encodes the catalytic subunit of aspartate carbamoyltransferase (ATCase); the other three genes were originally annotated as genes putatively encoding OTCase. However, one of these genes (EF0732) was recently recognized to have an encoded protein sequence that matches the previously published *N*-terminal PTCase sequence[5] and to be close to the gene cluster of the agmatine deiminase pathway[7,8]. Therefore, this gene and its close homologs in *Lactococcus lactis*, *Streptococcus mutans* and *Lactobacillus monocytogenes* were recently re-annotated as genes encoding PTCase[7,9]. Although the gene names for PTCase in the literatures and databases are not consistent[8], here we designate the PTCase gene as *agcB*, consistent with the convention used for the *arcABC* operon of the arginine catabolic pathway[10]. In *E. faecalis*, the primary sequence of PTCase contains 339 amino acids and has 48% sequence similarity to EF0105 encoded catabolic OTCase. The last carbamoyltransferase gene (EF2517) in the *E. faecalis* genome encodes a catabolic carbamoyltransferase of unknown function (UTCase) similar to the *ygeW* encoded carbamoyltransferase in the *E. coli* genome. The recent structural determination of the latter demonstrated that it has a unique 3_1 trefoil knot close to the proposed active site which is not present in ATCase and OTCase, but is present in *N*-acetylornithine (AOTCase) and *N*-succinylornithine carbamoyltransferase (SOTCase), suggesting that it is an ancestral catabolic carbamoyltransferase[11].

Although no crystal structure of PTCase has been reported beyond a report of crystallization[10], more than 27 structures have been reported for its close analog, OTCase, from multiple organisms, including *Escherichia coli* (ecOTCase)[12-14], *Pseudomonas aeruginosa*[15], *Pyrococcus furiosus*[16,17], *Mycobacterium tuberculosis*[18], *Lactobacillus hilgardii*[19], *Giardia lamblia*[20], sheep[21] and humans [21-24]. The functional molecular unit for most anabolic OTCases is a trimer, with the exception of OTCase from the hyperthermophilic bacterium *Py. furiosus* which is a dodecamer[17,25]. The oligomeric forms of catabolic OTCase are much more diverse: dodecameric in *Ps. aeruginosa*, hexameric in *L. hilgardii* and trimeric in *G. lamblia*. Catabolic PTCase from *E. faecalis* (efPTCase) has been reported to function as a trimer, as determined by gel filtration[4] and more recent studies have confirmed that recombinant efPTCase is also a highly stable trimer[10]. In contrast, the analogous catabolic OTCase from *E. faecalis* appears to be a hexamer[4].

The biochemical properties of efPTCase purified from cell extract have been studied[4]. In contrast to other members of the carbamoyltransferase family which have quite narrow

specificity towards their substrates, efPTCase has broad substrate specificity which enables it to carbamoylate putrescine, ornithine and several other diamines. However, putrescine is carbamoylated most efficiently. Recent studies of recombinant efPTCase confirmed that efPTCase has high PTCase and significant OTCase activity[10].

Here, we report the biochemical properties and crystal structure of catabolic efPTCase, which functions as a trimer and shows obvious cooperativity for both carbamoyl phosphate (CP) and putrescine. Since there are 12 subunits (four molecular trimers) in the asymmetric unit, averaging over the twelve fold non-crystallographic symmetry enables most of the structure to be well defined. The structure provides insights into the active site and the role of the *C*-terminal helix in maintaining a very stable trimer.

MATERIALS AND METHODS

Cloning and protein preparation

The *agcB* gene was PCR amplified from *E. faecalis* genomic DNA (ATCC 33913D), using hot-started turbo *pfu* DNA polymerase and the primer 5′-GACATATGACCGATCTACTCG-3′ and 5′-GCGAATTCCAGTGCGAGCCGTTGATG-3′. The PCR products were cloned into a Topo vector using a Zero-blunt Topo cloning kit (Invitrogen) with subsequent insertion into a pET28a vectors (Novagen) using T4 DNA ligase (New England BioLabs) and transformation into *E. coli* BL21(DE3) cells (Invitrogen) for overexpression. The protein was prepared using the overnight express auto-induction system 1 (Novagen) according to the manufacturer's protocol. Briefly, 1L LB media was supplemented with chemicals provided in the kit and cultures were grown overnight at 310 K. The cells were harvested by centrifugation, and suspended in 40 ml of Ni-affinity lysis buffer (300 mM NaCl, 50 mM NaH_2PO_4, pH 7.4, 10% (v/v) glycerol, 10 mM β-mercaptoethanol), and disrupted by sonication. The protein was purified first by Histrap Ni-affinity column (GE Healthcare) and then by Hightrap DEAE column (GE Healthcare) using an AKTA FPLC system. In the first step, the soluble fraction was loaded onto a 5 ml Histrap Ni-affinity column previously equilibrated with lysis buffer and then the column was washed with the buffer containing 50 mM imidazole. The protein was eluted with the buffer containing 250 mM imidazole. In the second step, the protein was dialyzed into buffer containing 50 mM NaCl, 20 mM Tris-HCl (pH 8.0), 1 mM EDTA and 5 mM β-mercaptoethanol. The protein was then loaded onto a DEAE Hightrap column and eluted using the linear gradient method applied against a buffer containing 500 mM NaCl, 20 mM Tris-HCl (pH 8.0), 1 mM EDTA and 5 mM β-mercaptoethanol. The protein was eluted out at 40 % (v/v) of target buffer. The protein purity was verified by SDS-PAGE (12% (v/v) polyacrylamide gel) followed by Coomassie staining. Protein concentration was determined by the Bradford method using BioRad protein assay dye reagent with bovine serum albumin as a standard[26].

Preparation of truncated PTCase

The expression vector for truncated PTCase without the *C*-terminal helix was prepared using site-directed mutagenesis to mutate the Glu313 codon to a stop codon using the Quik Change Mutagenesis Kit according to the manufacturer's protocol. The mutation was verified with an ABI PRISM 3130 Genetic Analyzer (Applied Biosystems) using the commercially available primer pair annealed to the plasmid promoter and terminator regions. Truncated PTCase was expressed and purified in the same way as wild-type PTCase, with minor modifications. The yield for truncated PTCase is ten fold lower than that for wild type PTCase.

Enzymatic assay

A colorimetric assay similar to that used to determine the activity of other carbamoyltransferases was modified to determine PTCase activity[11,27-30] by detecting the synthesis of carbamoylputrescine from CP and putrescine. The wild-type putrescine titration curve was obtained by incubating 0.2 μg of enzyme and varying amount of putrescine for 5 minutes at 295 K in a buffer containing 200 mM 3,3-dimethylglutaric acid, pH 6.9, and 1.0 mM of CP. The CP titration curve was determined in the same buffer with 5.0, 0.5 and 0.05 mM putrescine and varying amounts of CP. To keep the assay within the detection limit, 0.2, 2.0 and 20 μg of enzymes were used for the three concentrations, respectively. Assays of the truncated enzyme were carried out with 2.0 μg of enzyme. Since carbamoylputrescine is not commercially available, butylurea was used as a standard for the PTCase activity assay. The ornithine titration curve was obtained in the same buffer but with varying amounts of L-ornithine and 50 μg of enzyme.

Both the CP and putrescine titration curves were fit to the Hill equation. All non-linear fitting was performed using the program gnuplot (http://www.gnuplot.info/).

Cross-linking experiment

Cross-linking experiments were performed using the protocol described by Davies and Stark (1976)[31]. Wild type and truncated PTCase (0.15 μg) were incubated with the cross-linking reagent dimethyl suberimidate (0.25 μg) in 50 μl of a solution containing 200 mM triethanolamine, pH 8.25 overnight at 277 K. Samples with and without cross-linking reagent were subjected to sodium dodecyl sulfate polyacrylamide gel electrophoresis (SDS-PAGE) and stained with Coomassie blue.

Analytic gel filtration chromatography

Analytic gel filtration experiments were performed using a Superdex 200HR (10/30) column mounted on an AKTA fast protein liquid chromatography system (GE Healthcare) as described previously[32]. A solution of 100 mM NaCl, 50 mM Tris-HCl pH 8.5 was used as the mobile phase, running at a flow rate of 1.0 ml/min. Molecular weight standard protein markers (Amersham Biosciences) consisted of aldolase, catalase, ferritin, thyroglobulin, blue dextran 2000, ribonuclease A, chymotrypsinogen, ovalbumin and albumin.

Crystallization and data collection

The purified protein was concentrated to ~10 mg/ml with an Amicon-Y30 membrane concentrator (Millipore) and the Hampton Research index screening kit was used to identify initial crystallization conditions at 291 K. After optimization, the best crystals, which diffract to about 3.2 Å resolution and have a maximum dimension of 0.1 mm were grown from a solution containing 200 mM magnesium sulfate, 15-17% (w/v) PEG 3350, 100 mM bis-tris, pH 5.5. Extensive efforts to prepare crystals that diffracted to a higher resolution data with and without substrate bound and with and without a his-tag were not successful. The best crystals belong to space group *C*2 and have unit cell parameters of a = 273.48, b = 87.74, c=240.69 Å and β=114.08°. Even though the packing-density calculation[33] for a monomer with molecular weight of 40 kDa indicated the presence of 12 monomers in the asymmetric unit (V_M = 2.74 $Å^3$ Da^{-1}, solvent content of 54.8%), the statistics of reflections after indexing indicated that a higher symmetric space group with different unit cell parameters is unlikely.

Before data collection, a crystal was dipped in a solution of 200 mM magnesium sulfate, 17% (w/v) PEG 3350, 100 mM bis-tris pH 5.5 supplemented by 25% (v/v) ethylene glycol for less than one minute for cryoprotection. The cryoprotected crystal was frozen by plunging it directly into liquid nitrogen. A data set to 3.2 Å resolution was collected with

synchrotron source X29A at Brookhaven National Laboratory. Data were processed using the HKL2000 package[34] and are summarized in Table 1.

Structural determination and refinement

The structure was determined by molecular replacement using the program Phaser[35,36] and the trimeric structure of OTCase from *Py. furiosus*[16] (PDB accession code 1PVV) as a search model. Phasing was greatly improved by 12 fold non-crystallographic symmetry averaging. After the first run of model building and rigid-body refinement, the *C*-terminal helix was visible in the electron density map and built into the model. Interestingly, partial sequences of the *N*-terminal his_6 tags that were incorporated into the construct to facilitate protein purification are visible in subunits B, D and E and were included in the structural model. The model was refined to R = 19.0 % (R_{free} = 23.4%) and has good geometry, as defined by PROCHECK[37] (Table1). Despite the 3.2 Å resolution, the quality of the electron density is comparable (Fig. 1) to other structures at similar resolution because of the symmetry averaging and the real space "R-factor" fit of the density to every residue is reasonable, except in the flexible 80's and 240's loops (Supplementary Information, Fig. S1). Atomic coordinates and structure factors have been deposited in Protein Data Bank (accession number 3TXX).

Figures 4 and 6 were drawn using programs Pymol[38]. Figure 5 was drawn using program ALSCRIPT[39]. The secondary structure was assigned using the STRIDE web server[40].

RESULTS AND DISCUSSION

Kinetics properties of efPTCase

In most carbamoyltransferases, substrate binding is ordered with CP binding first[24,41,42], and in some carbamoyltransferases binding of a substrate is cooperative. Examples include hexameric *E. coli* ATCase, which undergoes a major change in quaternary structure from the T to R state when its second substrate, L-Asp, binds[43,44] and dodecameric catabolic OTCase from *Ps. aeruginosa* which binds its first substrate, CP, cooperatively[45].

Although trimeric OTCases generally do not bind substrates cooperatively, efPTCase binds putrescine with obvious cooperativity, with a Hill coefficient of 1.80 ± 0.06, K_m of 0.136 ± 0.003 mM, and V_{max} of 17.68 ± 0.13 μmol/min/mg at saturating concentrations of CP (Fig. 2B). efPTCase also appears to bind CP cooperatively, with a Hill coefficient of 1.53 ± 0.03, K_m of 0.101 ± 0.001 mM, and V_{max} of 148.8 ± 1.0 μmol/min/mg (Fig. 2A) at saturating concentrations of putrescine (5.0 mM). However, *E. coli* ATCase also appeared to bind CP cooperatively at saturating concentrations of L-Asp because its binding is linked to L-Asp binding through the T to R transition. At low L-Asp concentrations, where *E.coli* ATCase remains in the T state, CP does not appear to bind cooperatively[46]. To determine whether efPTCase behaves similarly, CP titration curves were obtained at two non-saturating concentrations of putrescine (0.5 and 0.05 mM). Interestingly, CP displays even higher cooperativity at these concentrations, with Hill coefficients of 1.87 ± 0.06 and 2.42 ± 0.17, respectively (Fig. 2C and 2D). Although the cooperative binding of both CP and putrescine to efPTCase may be related to the strong intersubunit interactions generated by the unique *C*-terminal helix in PTCase, the structural basis of this cooperativity can be elucidated only when crystals with the bound ligand have been obtained.

As mentioned earlier, PTCase catalyzes the carbamoylation of ornithine less efficiently, with a K_m of 23.3 ± 1.7 mM and V_{max} of 0.24 ± 0.01 μmol/min/mg for ornithine (Supplementary Information, Fig. S2). These results are consistent with earlier studies by Warngies (1979)[4]. Truncated PTCase, which lacks the *N*-terminal helix has significantly lower specific

activity: 1.5 ± 0.2 μmol/min/mg, relative to 32.4 ± 3.5 μmol/min/mg for wild type PTCase assayed under the same conditions.

The *C*-terminal helix is essential for the formation of functional trimer

Cross-linking experiments that show three major bands, with molecular weights corresponding to oligomers of 1, 2, 3 subunits confirm that wild-type PTCase exists primarily as a trimer in solution (Fig. 3A). However, in addition to the major band corresponding to the monomer, at least six faint bands corresponding to higher oligomers were observed for truncated PTCase. Analytic gel filtration experiments are consistent with wild type PTCase eluting at a position corresponding to the trimer (Fig. 3B), and truncated PTCase eluting in the void volume (Fig. 3B), indicating that PTCase exists primarily as higher oligomers in solution. The higher oligomers for truncated PTCase are probably random aggregates since no dominant bands were observed in cross-linking experiments. Clearly the *C*-terminal helix is important for maintaining functional trimers.

Monomer structure

As in other carbamoyltransferases, the monomer of efPTCase, which consists of 393 amino acid residues, is composed of two domains: the CP binding domain and the second substrate domain which binds putrescine. Both the CP and PTC binding domains exhibit α/β topology with a central parallel β-sheet as the core, flanked by α-helices on both sides. Two interdomain helices (H5 and H11) connect the two domains, and the active site is located in the cleft between the two domains. The distinctive feature of efPTCase is a *C*-terminal helix (H12) separated from the rest of the structure by a long loop (Fig. 4B) that is involved in the formation of the molecular trimer (Fig. 4A) as described in the following section.

A DALI search[47] identified OTCase from *Py. furiosus* as the most closely related structure with a Z-score of 43.3 and root mean square deviation (RMSD) of 1.3 Å for 313 aligned α-carbon atoms that share 46% sequence identity (accession code 1A1S). OTCase structures from other organisms have Z-scores of 37-43 and RMSD values of 1.3-1.9 Å. AOTCase structures have the next highest degree of structural similarity, with Z scores of approximately 36 and RMSD values of approximately 2.0 Å. ATCase structures have Z scores of 31.7-32.5 and RMSD values of 2.0-2.5 Å. SOTCase appears to be a more distantly related member of the carbamoyltransferase family, with a Z score of 31.4 and RMSD of 2.5 Å. The recently determined *ygeW* encoded carbamoyltransferase[11] (PDB accession code 3Q98) is the most distant member of the carbamoyltransferase family relative to PTCase, with a Z score of 30.3 and a RMSD value of 2.4 Å.

Like OTCases and ATCases, PTCase has neither a proline-rich loop nor a knotted fold, in contrast to AOTCase, SOTCase and *ygeW* encoded UTCase, which have both features[11,30,48]. Thus the structure of PTCase is further confirmation that a proline-rich loop is a prerequisite for knot formation in carbamoyltransferases[49,50].

Interactions between subunits within trimers

The trimer of efPTCase has an approximate width of 90 Å and thickness of 55 Å (Fig. 4A). The structure of the trimer is similar to other carbamoyltransferases, with the CP-binding domains close to the center of the trimer and the putrescine binding domains closer to the surface. The buried interface area between two adjacent subunits is 1865 $Å^2$, calculated by the PISA server[51], much larger than for other carbamoyltransferases (Supplementary Information, Table S1). The long *C*-terminal helix contributes about 820 $Å^2$ buried surface area.

His-tags are involved in the crystal packing

Pair-wise secondary structural alignment of the twelve subunits in the asymmetric unit (Supplementary Information, Fig. S3) yields an RMSD of ~0.05 Å for equivalent Cα atoms. The small RMSD values result in part from using non-crystallography symmetry (NCS) restraints. However, the low *R* value from the refinements suggests that the subunit structures are indeed quite similar and that their conformations are not affected by different packing environments in the crystal. Among the 12 subunits in an asymmetric unit, two subunits (subunits B and E) have significant electron density at their *N*-termini that can be modeled as the leading sequence (His-tag and thrombin cleavage site) from the cloning vector (Supplementary Information, Fig. S4). The leading uncleaved His tags of subunit B and E protrude into the active site of subunit B and E from the adjacent molecular trimers (Supplementary Information Fig. S4) and thus are involved in the molecular packing. Crystal structures that include His-tags have increasingly been detected, although the tagged sequence can be fit into density in less than 10% of structures[52]. Generally, His-tags do not have a significant effect on the structure of the native protein.

Active site and substrate binding

Superimposition of the efPTCase structure with the OTCase structure from *E. coli* (accession code, 1DUV) demonstrates that their active sites are very similar (Fig. 6B), consistent with the ability of efPTCase to catalyze the carbamoylation of both putrescine and ornithine. In the efPTCase structure, there is extra electron density in the proposed CP binding site in all subunits that could be modeled as one or two sulfate groups with hydrogen bonding networks similar to those in the CP binding site of OTCase (Fig. 6A). Two phosphate groups that are analogous to these sulfate groups have been observed in ATCase structures[53] and docking experiment indicate that these sites may represent possible entry or exit routes for phosphate[54]. Most of the active site residues in efPTCase and ecOTCase are the same except for differences in the 240's loop of efPTCase and the corresponding SMG loop in ecOTCase. The only other difference is in Gln164, which is replaced by Asn167 in ecOTCase. Since PTCases in other bacteria also have an Asn in this position, this residue may not be important to determining the substrate specificity of PTCases.

Because both PTCase and OTCase structures are unknotted structures, the 240's loop (residues 227 to 251) in efPTCase would be able to swing into the active site so as to be able to interact with the second substrate (putrescine for PTCase) as does the SMG loop in OTCase structures[12,23]. ecOTCase uses D231, S235 and Met236 (*E. coli* OTCase numbering) in the 240's loop and Asn167 to bind the α-amino and carboxyl groups of ornithine. The equivalent second substrate binding residues for efPTCase are D227, Gly231 and Leu232 in the 240's loop and Gln164. The side-chains of D227 and Gln164 are oriented so as to be able to hydrogen bond with the amino group of putrescine. Since Gly231 has no side-chain, its main-chain O may be involved in hydrogen bonding to the amino group of putrescine. The side chain of Leu232 seems likely to have hydrophobic interactions with the hydrophobic stem of putrescine as does the side chain of Met236 in ecOTCase. Since putrescine does not have a carboxyl group, the 240's loop in PTCase can swing a larger distance into the active site (1.0-1.5 Å) than the SMG loop of OTCase to enable hydrogen bonding interactions with the amino group of putrescine.

PTCase genes in bacteria

A BLAST search of protein sequences in the NBCI database identified 35 species, primarily Gram-positive bacteria, that have *agcB* or *agcB*-like genes that would be expected to encode PTCase (Supplementary Information, Table S2). Gram-negative bacteria usually have *aguB* genes encoding *N*-carbamoylputrescine amidohydrolase which catalyzes the conversion of

N-carbamoylputrescine to putrescine, carbon dioxide and ammonium[55]. The gene name *aguB* has sometimes been used to designate the gene encoding PTCase as well[7,9]. In fact, PTCase is neither homologous nor analogous to *N*-carbamoylputrescine amidohydrolase, even though both convert carbamoylputrescine to putrescine.

There is usually only one *agcB* gene per genome, however, there are two *agcB*-like genes in *Slackia exidgus* ATCC 700122, a saccharolytic anaerobic Gram-positive bacteria predominant in the oral cavity[56,57]. The similarity between these two PTCase-like proteins (ZP_06160210 and ZP_06160597) is 69%. Whether both proteins play a catabolic role in agmatine degradation pathway remains to be determined.

A protein sequence alignment for PTCase is provided in the Supporting Information (Fig. S5). Pair-wise sequence comparison indicates that the sequence identities of pairs of PTCases from different species are between 45% and 80%. All PTCase sequences have an extra sequence encoding an extra *C*-terminal α-helix. In some species such as *Mycoplasma capricolum* and *Brevundimonas sp.* BAL3, the *C*-terminal helix is 15-20 residues longer than in efPTCase. The additional *C*-terminal sequence appears to be the signature feature of PTCase (Fig. 5). Since this extra *C*-terminal α-helix is located on the convex surface of the trimer, it may also be involved in mediating interactions with the downstream enzyme, CK, or channeling the thermolabile metabolite, CP, although this remains to be investigated. However, OTCase forms a complex with CK in the thermophile*, Py. furiosus,* that promotes CP channeling[58,59].

Gene context analysis for all available genomes with the *agcB* gene indicates that the *agcB* gene is usually located adjacent to *agcA*, which encodes agmatine deiminase, and *agcC*, which encodes carbamate kinase, as reported previously[7,9] (Supplementary Information, Table S2).

The ability of catabolic carbamoyltransferases to function in the thermodynamically unfavorable direction *in vivo* does not appear to be correlated with its oligomeric state, affinity for CP, or cooperativity. The critical factor is instead coupling to CK, which allows CP produced by catabolic carbamoyltransferases operating in the reverse direction to be immediately consumed by CK to form ATP. Co-location of catabolic carbamoyltransferase genes and CK genes in the same operon, so that they can be co-transcribed, as is the case with PTCase, catabolic OTCase and even UTCase, is consistent with this coupling[11].

Distinguishing PTCase from other carbamoyltransferases

Since the sequence similarity between PTCase and OTCase may be as high as 48%, it is easy to mis-annotate PTCase as OTCase, AOTCase, or SOTCase if the annotation is based only on sequence comparisons[7]. With structures of all four enzymes now available, additional criteria can be used. As noted above, the extra *C*-terminal helix, and its involvement in formation of PTCase catalytic trimer, seems to be specific to PTCase. (Although UTCase also has an extra *C*-terminal helix, its helix is shorter than that of PTCase and does not extend to the adjacent subunit[11]). In addition, PTCase is an unknotted carbamoyltransferase and, unlike AOTCase, SOTCase and UTCase, does not have a proline-rich loop. The 240's loop of PTCase, whose equivalent loops in other carbamoyltransferases are major recognition sites for the second substrate, appears to be less conserved than in OTCase and ATCase, probably because it uses main-chain oxygen to hydrogen bond with the amino group of putrescine. The PTCase gene seems to be always near the gene that encodes agmatine deiminase, just as the catabolic OTCase gene is next to the gene that encodes arginine deiminase. However, PTCase can be readily distinguished from OTCase in most bacterial genomics, because the protein sequences and three-dimensional structures of agmatine deiminase and arginine deiminase are significantly different. Agmatine deiminase

lacks the five-helix bundle domain of arginine deiminase and its sequence is 150 amino acid residues shorter than that of arginine deiminase[10,60]. A carbamoyltransferase gene near an agmatine deiminase gene is likely to be an PTCase, not a OTCase.

Does PTCase functions as catabolic OTCase in vivo in some bacteria?

Although PTCase is most efficient in catalyzing the carbamoylation of putrescine to carbamoylputrescine, it has significant OTCase activity, in contrast to other carbamoyltransferases that have very specific carbamoyltransferase activity. Recently, PTCase in *Listeria monocytogenes* EGD-e (encoded by lmo0036) was shown to function as a catabolic enzyme in both arginine and agmatine degradation pathways and to play an important role in enabling the bacterium to tolerate acidic conditions[61]. Indeed, in the *L. monocytogenes* EGD-e genome, the PTCase gene lmo0036 is next to the genes thatencode both agmatine deiminase (lmo0038 and lmo0040) and arginine deiminase (lmo0043). Thus PTCase may be an example of a promiscuous enzyme that is able to function as both a catabolic PTCase and a catabolic OTCase in some bacteria.

Supplementary Material

Refer to Web version on PubMed Central for supplementary material.

Acknowledgments

The authors thank David Davies and Fred Dyda for facilitating use of the diffraction equipment in the Molecular Structure Section of the National Institute of Health. This work was supported by Public Health Service grant DK-47870 (to M. T.) and DK-067935 (to D. S.) from the National Institute of Diabetes, Digestive and Kidney Diseases. Use of the National Synchrotron Light Source, Brookhaven National Laboratory, was supported by the U.S. Department of Energy, Office of Science, Office of Basic Energy Sciences, under Contract No. DE-AC02-98CH10886.

Abbreviations

ADI	arginine deiminase
AgDI	agmatine deiminase
AOTCase	acetyl-ornithine carbamoyltransferase
ATCase	aspartate carbamoyltransferase
CK	carbamate kinase
CP	carbamoyl phosphate
ecOTCase	*Escherichia coli* ornithine carbamoyltransferase
efPTCase	*Enterococcus faecalis* putrescine carbamoyltransferase
OTCase	ornithine carbamoyltransferase
PTCase	putrescine carbamoyltransferase
RMSD	root mean square deviation
SOTCase	*N*-succinyl-ornithine carbamoyltransferase
UTCase	carbamoyltransferase of unknown function

REFERENCES

1. Cunin R, Glansdorff N, Pierard A, Stalon V. Biosynthesis and metabolism of arginine in bacteria. Microbiol Rev. 1986; 50(3):314–352. [PubMed: 3534538]

2. Jones ME, Lipmann F. Chemical and Enzymatic Synthesis of Carbamyl Phosphate. Proc Natl Acad Sci U S A. 1960; 46(9):1194–1205. [PubMed: 16590733]
3. Roon RJ, Barker HA. Fermentation of agmatine in Streptococcus faecalis: occurrence of putrescine transcarbamoylase. J Bacteriol. 1972; 109(1):44–50. [PubMed: 4621632]
4. Wargnies B, Lauwers N, Stalon V. Structure and properties of the putrescine carbamoyltransferase of Streptococcus faecalis. Eur J Biochem. 1979; 101(1):143–152. [PubMed: 116850]
5. Tricot C, De Coen JL, Momin P, Falmagne P, Stalon V. Evolutionary relationships among bacterial carbamoyltransferases. J Gen Microbiol. 1989; 135(9):2453–2464. [PubMed: 2516870]
6. Paulsen IT, Banerjei L, Myers GS, Nelson KE, Seshadri R, Read TD, Fouts DE, Eisen JA, Gill SR, Heidelberg JF, Tettelin H, Dodson RJ, Umayam L, Brinkac L, Beanan M, Daugherty S, DeBoy RT, Durkin S, Kolonay J, Madupu R, Nelson W, Vamathevan J, Tran B, Upton J, Hansen T, Shetty J, Khouri H, Utterback T, Radune D, Ketchum KA, Dougherty BA, Fraser CM. Role of mobile DNA in the evolution of vancomycin-resistant Enterococcus faecalis. Science. 2003; 299(5615):2071–2074. [PubMed: 12663927]
7. Naumoff DG, Xu Y, Glansdorff N, Labedan B. Retrieving sequences of enzymes experimentally characterized but erroneously annotated : the case of the putrescine carbamoyltransferase. BMC Genomics. 2004; 5(1):52. [PubMed: 15287962]
8. Naumoff DG, Xu Y, Stalon V, Glansdorff N, Labedan B. The difficulty of annotating genes: the case of putrescine carbamoyltransferase. Microbiology. 2004; 150(Pt 12):3908–3911. [PubMed: 15583144]
9. Griswold AR, Chen YY, Burne RA. Analysis of an agmatine deiminase gene cluster in Streptococcus mutans UA159. J Bacteriol. 2004; 186(6):1902–1904. [PubMed: 14996823]
10. Llacer JL, Polo LM, Tavarez S, Alarcon B, Hilario R, Rubio V. The gene cluster for agmatine catabolism of Enterococcus faecalis: study of recombinant putrescine transcarbamylase and agmatine deiminase and a snapshot of agmatine deiminase catalyzing its reaction. J Bacteriol. 2007; 189(4):1254–1265. [PubMed: 17028272]
11. Li Y, Jin Z, Yu X, Allewell NM, Tuchman M, Shi D. The ygeW encoded protein from Escherichia coli is a knotted ancestral catabolic transcarbamylase. Proteins. 2011; 79(7):2327–2334. [PubMed: 21557323]
12. Ha Y, McCann MT, Tuchman M, Allewell NM. Substrate-induced conformational change in a trimeric ornithine transcarbamoylase. Proc Natl Acad Sci U S A. 1997; 94(18):9550–9555. [PubMed: 9275160]
13. Jin L, Seaton BA, Head JF. Crystal structure at 2.8 A resolution of anabolic ornithine transcarbamylase from Escherichia coli. Nat Struct Biol. 1997; 4(8):622–625. [PubMed: 9253409]
14. Langley DB, Templeton MD, Fields BA, Mitchell RE, Collyer CA. Mechanism of inactivation of ornithine transcarbamoylase by Ndelta -(N'-Sulfodiaminophosphinyl)-L-ornithine, a true transition state analogue? Crystal structure and implications for catalytic mechanism. J Biol Chem. 2000; 275(26):20012–20019. [PubMed: 10747936]
15. Villeret V, Tricot C, Stalon V, Dideberg O. Crystal structure of Pseudomonas aeruginosa catabolic ornithine transcarbamoylase at 3.0-A resolution: a different oligomeric organization in the transcarbamoylase family. Proc Natl Acad Sci U S A. 1995; 92(23):10762–10766. [PubMed: 7479879]
16. Massant J, Wouters J, Glansdorff N. Refined structure of Pyrococcus furiosus ornithine carbamoyltransferase at 1.87 A. Acta Crystallogr D Biol Crystallogr. 2003; 59(Pt 12):2140–2149. [PubMed: 14646072]
17. Villeret V, Clantin B, Tricot C, Legrain C, Roovers M, Stalon V, Glansdorff N, Van Beeumen J. The crystal structure of Pyrococcus furiosus ornithine carbamoyltransferase reveals a key role for oligomerization in enzyme stability at extremely high temperatures. Proc Natl Acad Sci U S A. 1998; 95(6):2801–2806. [PubMed: 9501170]
18. Sankaranarayanan R, Cherney MM, Cherney LT, Garen CR, Moradian F, James MN. The crystal structures of ornithine carbamoyltransferase from Mycobacterium tuberculosis and its ternary complex with carbamoyl phosphate and L-norvaline reveal the enzyme's catalytic mechanism. J Mol Biol. 2008; 375(4):1052–1063. [PubMed: 18062991]

19. de Las Rivas B, Fox GC, Angulo I, Ripoll MM, Rodriguez H, Munoz R, Mancheno JM. Crystal structure of the hexameric catabolic ornithine transcarbamylase from Lactobacillus hilgardii: Structural insights into the oligomeric assembly and metal binding. J Mol Biol. 2009; 393(2):425–434. [PubMed: 19666033]
20. Galkin A, Kulakova L, Wu R, Gong M, Dunaway-Mariano D, Herzberg O. X-ray structure and kinetic properties of ornithine transcarbamoylase from the human parasite Giardia lamblia. Proteins. 2009; 76(4):1049–1053. [PubMed: 19507245]
21. De Gregorio A, Battistutta R, Arena N, Panzalorto M, Francescato P, Valentini G, Bruno G, Zanotti G. Functional and structural characterization of ovine ornithine transcarbamoylase. Org Biomol Chem. 2003; 1(18):3178–3185. [PubMed: 14527149]
22. Shi D, Morizono H, Aoyagi M, Tuchman M, Allewell NM. Crystal structure of human ornithine transcarbamylase complexed with carbamoyl phosphate and L-norvaline at 1.9 A resolution. Proteins. 2000; 39(4):271–277. [PubMed: 10813810]
23. Shi D, Morizono H, Ha Y, Aoyagi M, Tuchman M, Allewell NM. 1.85-A resolution crystal structure of human ornithine transcarbamoylase complexed with N-phosphonacetyl-L-ornithine. Catalytic mechanism and correlation with inherited deficiency. J Biol Chem. 1998; 273(51): 34247–34254. [PubMed: 9852088]
24. Shi D, Morizono H, Yu X, Tong L, Allewell NM, Tuchman M. Human ornithine transcarbamylase: crystallographic insights into substrate recognition and conformational changes. Biochem J. 2001; 354(Pt 3):501–509. [PubMed: 11237854]
25. Clantin B, Tricot C, Lonhienne T, Stalon V, Villeret V. Probing the role of oligomerization in the high thermal stability of Pyrococcus furiosus ornithine carbamoyltransferase by site-specific mutants. Eur J Biochem. 2001; 268(14):3937–3942. [PubMed: 11453986]
26. Bradford MM. A rapid and sensitive method for the quantitation of microgram quantities of protein utilizing the principle of protein-dye binding. Anal Biochem. 1976; 72:248–254. [PubMed: 942051]
27. Morizono H, Cabrera-Luque J, Shi D, Gallegos R, Yamaguchi S, Yu X, Allewell NM, Malamy MH, Tuchman M. Acetylornithine transcarbamylase: a novel enzyme in arginine biosynthesis. J Bacteriol. 2006; 188(8):2974–2982. [PubMed: 16585758]
28. Morizono H, Tuchman M, Rajagopal BS, McCann MT, Listrom CD, Yuan X, Venugopal D, Barany G, Allewell NM. Expression, purification and kinetic characterization of wild-type human ornithine transcarbamylase and a recurrent mutant that produces ‘late onset’ hyperammonaemia. Biochem J. 1997; 322(Pt 2):625–631. [PubMed: 9065786]
29. Pastra-Landis SC, Foote J, Kantrowitz ER. An improved colorimetric assay for aspartate and ornithine transcarbamylases. Anal Biochem. 1981; 118(2):358–363. [PubMed: 7337232]
30. Shi D, Morizono H, Cabrera-Luque J, Yu X, Roth L, Malamy MH, Allewell NM, Tuchman M. Structure and catalytic mechanism of a novel N-succinyl-L-ornithine transcarbamylase in arginine biosynthesis of Bacteroides fragilis. J Biol Chem. 2006; 281(29):20623–20631. [PubMed: 16704984]
31. Davies GE, Stark GR. Use of dimethyl suberimidate, a cross-linking reagent, in studying the subunit structure of oligomeric proteins. Proc Natl Acad Sci U S A. 1970; 66(3):651–656. [PubMed: 4913206]
32. Shi D, Sagar V, Jin Z, Yu X, Caldovic L, Morizono H, Allewell NM, Tuchman M. The crystal structure of N-acetyl-L-glutamate synthase from Neisseria gonorrhoeae provides insights into mechanisms of catalysis and regulation. J Biol Chem. 2008; 283(11):7176–7184. [PubMed: 18184660]
33. Matthews BW. Solvent content of protein crystals. J Mol Biol. 1968; 33(2):491–497. [PubMed: 5700707]
34. Otwinowski Z, Minor W. Processing of X-ray diffraction data collected in oscillation mode. Methods Enzymol. 1997; 276:307–326.
35. Read RJ. Pushing the boundaries of molecular replacement with maximum likelihood. Acta Crystallogr D Biol Crystallogr. 2001; 57(Pt 10):1373–1382. [PubMed: 11567148]
36. Storoni LC, McCoy AJ, Read RJ. Likelihood-enhanced fast rotation functions. Acta Crystallogr D Biol Crystallogr. 2004; 60(Pt 3):432–438. [PubMed: 14993666]

37. Laskowski RA, MacArthur NW, Moss DS, Thornton JM. PROCHECK: a program to check the stereochemical quality of protein structures. J Appl Crystallogr. 1993; 26:283–291.
38. Schrodinger, L. The PyMOL Molecular Graphics System. Version 1.3r1. 2010.
39. Barton GJ. ALSCRIPT: a tool to format multiple sequence alignments. Protein Eng. 1993; 6(1): 37–40. [PubMed: 8433969]
40. Heinig M, Frishman D. STRIDE: a web server for secondary structure assignment from known atomic coordinates of proteins. Nucleic Acids Res. 2004; 32(Web Server issue):W500–502. [PubMed: 15215436]
41. Goldsmith JO, Kuo LC. Utilization of conformational flexibility in enzyme action-linkage between binding, isomerization, and catalysis. J Biol Chem. 1993; 268(25):18481–18484. [PubMed: 8360150]
42. Porter RW, Modebe MO, Stark GR. Aspartate transcarbamylase. Kinetic studies of the catalytic subunit. J Biol Chem. 1969; 244(7):1846–1859. [PubMed: 4889008]
43. Kantrowitz ER, Lipscomb WN. Escherichia coli aspartate transcarbamoylase: the molecular basis for a concerted allosteric transition. Trends Biochem Sci. 1990; 15(2):53–59. [PubMed: 2186515]
44. Knier BL, Allewell NM. Calorimetric analysis of aspartate transcarbamylase from Escherichia coli. Binding of substrates and substrate analogues to the native enzyme and catalytic subunit. Biochemistry. 1978; 17(5):784–790. [PubMed: 343809]
45. Nguyen VT, Baker DP, Tricot C, Baur H, Villeret V, Dideberg O, Gigot D, Stalon V, Haas D. Catabolic ornithine carbamoyltransferase of Pseudomonas aeruginosa. Importance of the N-terminal region for dodecameric structure and homotropic carbamoylphosphate cooperativity. Eur J Biochem. 1996; 236(1):283–293. [PubMed: 8617277]
46. England P, Leconte C, Tauc P, Herve G. Apparent cooperativity for carbamoylphosphate in Escherichia coli aspartate transcarbamoylase only reflects cooperativity for aspartate. Eur J Biochem. 1994; 222(3):775–780. [PubMed: 8026491]
47. Holm L, Rosenstrom P. Dali server: conservation mapping in 3D. Nucleic Acids Res. 2011; 38(Web Server issue):W545–549. [PubMed: 20457744]
48. Shi D, Morizono H, Yu X, Roth L, Caldovic L, Allewell NM, Malamy MH, Tuchman M. Crystal structure of N-acetylornithine transcarbamylase from Xanthomonas campestris: a novel enzyme in a new arginine biosynthetic pathway found in several eubacteria. J Biol Chem. 2005; 280(15): 14366–14369. [PubMed: 15731101]
49. Potestio R, Micheletti C, Orland H. Knotted vs. unknotted proteins: evidence of knot-promoting loops. PLoS Comput Biol. 2010; 6(7):e1000864. [PubMed: 20686683]
50. Shi D, Yu X, Cabrera-Luque J, Chen TY, Roth L, Morizono H, Allewell NM, Tuchman M. A single mutation in the active site swaps the substrate specificity of N-acetyl-L-ornithine transcarbamylase and N-succinyl-L-ornithine transcarbamylase. Protein Sci. 2007; 16(8):1689–1699. [PubMed: 17600144]
51. Krissinel E, Henrick K. Inference of macromolecular assemblies from crystalline state. J Mol Biol. 2007; 372(3):774–797. [PubMed: 17681537]
52. Carson M, Johnson DH, McDonald H, Brouillette C, Delucas LJ. His-tag impact on structure. Acta Crystallogr D Biol Crystallogr. 2007; 63(Pt 3):295–301. [PubMed: 17327666]
53. Mendes KR, Kantrowitz ER. A cooperative Escherichia coli aspartate transcarbamoylase without regulatory subunits. Biochemistry. 2010; 49(35):7694–7703. [PubMed: 20681545]
54. Harris KM, Cockrell GM, Puleo DE, Kantrowitz ER. Crystallographic snapshots of the complete catalytic cycle of the unregulated aspartate transcarbamoylase from Bacillus subtilis. J Mol Biol. 2011; 411(1):190–200. [PubMed: 21663747]
55. Landete JM, Arena ME, Pardo I, Manca de Nadra MC, Ferrer S. The role of two families of bacterial enzymes in putrescine synthesis from agmatine via agmatine deiminase. Int Microbiol. 2010; 13(4):169–177. [PubMed: 21404211]
56. Booth V, Downes J, Van den Berg J, Wade WG. Gram-positive anaerobic bacilli in human periodontal disease. J Periodontal Res. 2004; 39(4):213–220. [PubMed: 15206913]
57. Uematsu H, Sato N, Djais A, Hoshino E. Degradation of arginine by Slackia exigua ATCC 700122 and Cryptobacterium curtum ATCC 700683. Oral Microbiol Immunol. 2006; 21(6):381–384. [PubMed: 17064396]

58. Massant J, Glansdorff N. New experimental approaches for investigating interactions between Pyrococcus furiosus carbamate kinase and carbamoyltransferases, enzymes involved in the channeling of thermolabile carbamoyl phosphate. Archaea. 2005; 1(6):365–373. [PubMed: 16243776]

59. Massant J, Verstreken P, Durbecq V, Kholti A, Legrain C, Beeckmans S, Cornelis P, Glansdorff N. Metabolic channeling of carbamoyl phosphate, a thermolabile intermediate: evidence for physical interaction between carbamate kinase-like carbamoyl-phosphate synthetase and ornithine carbamoyltransferase from the hyperthermophile Pyrococcus furiosus. J Biol Chem. 2002; 277(21):18517–18522. [PubMed: 11893735]

60. Das K, Butler GH, Kwiatkowski V, Clark AD Jr. Yadav P, Arnold E. Crystal structures of arginine deiminase with covalent reaction intermediates; implications for catalytic mechanism. Structure. 2004; 12(4):657–667. [PubMed: 15062088]

61. Chen J, Cheng C, Xia Y, Zhao H, Fang C, Shan Y, Wu B, Fang W. Lmo0036, an ornithine and putrescine carbamoyltransferase in Listeria monocytogenes, participates in arginine deiminase and agmatine deiminase pathways and mediates acid tolerance. Microbiology. 2011; 157:3150–3161. [PubMed: 21835877]

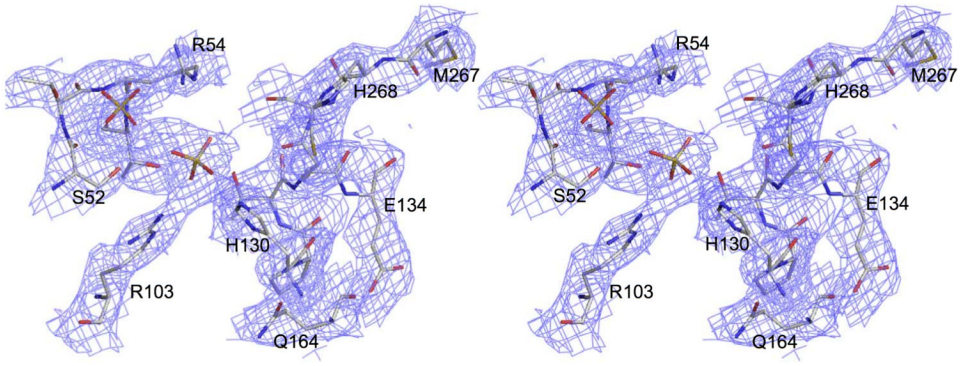

Figure 1.

Electron density map around the active site of subunit B. The electron density map (*2Fo-Fc*) contoured at 1.0 σ is shown as blue cages. Active site residues and two bound sulfate groups are shown as sticks.

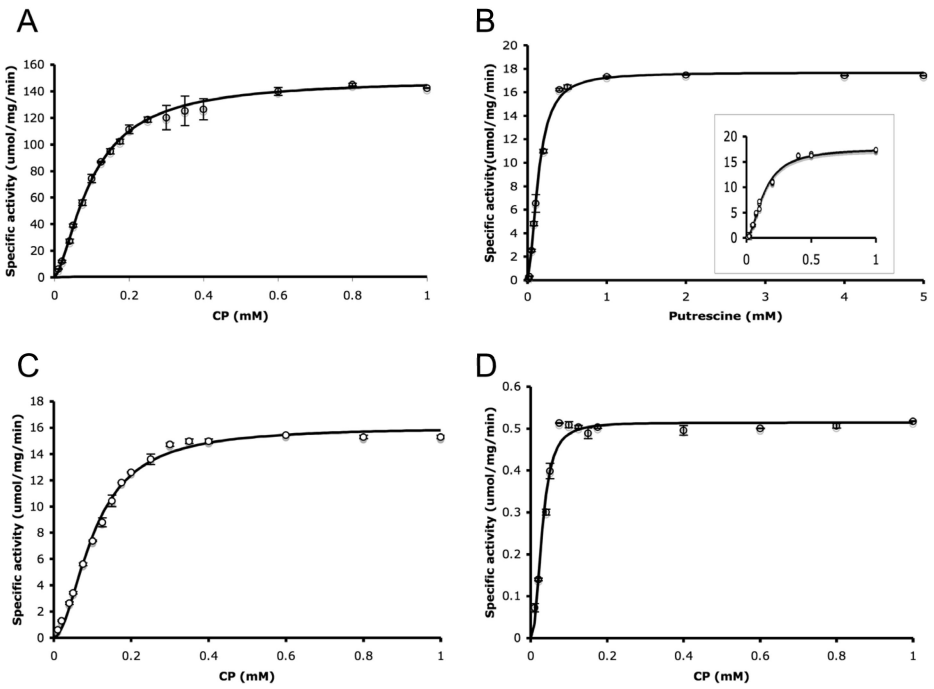

Figure 2.

Biochemical properties of efPTCase. *A*. Dependence of PTCase activity on the concentration of CP which was varied in the range of 0-1.0 mM with putrescine fixed at 5.0 mM. The calculated kinetic parameters are V_{max} = 148.8 ± 1.0 μmol/min/mg and K_m = 0.101 ± 0.001 mM and a Hill coefficient of 1.53 ± 0.03. *B*. Dependence of PTCase activity on the concentration of putrescine which was varied in the range of 0-5 mM in the presence of 1.0 mM of CP. The calculated kinetic parameters are V_{max} = 17.68 ± 0.06 μmol/min/mg and K_m = 0.136 ± 0.003 mM and a Hill coefficient of 1.80 ± 0.06. *C*. Dependence of PTCase activity on the concentration of CP which was varied in the range of 0-1.0 mM with putrescine fixed at 0.5 mM. The calculated kinetic parameters are V_{max} = 16.0 ± 0.2 μmol/min/mg and K_m = 0.104 ± 0.002 mM and a Hill coefficient of 1.87 ± 0.06. *D*. Dependence of PTCase activity on the concentration of CP which was varied in the range of 0-1.0 mM with putrescine fixed at 0.05 mM. The calculated kinetic parameters are V_{max} = 0.514 ± 0.6 μmol/min/mg and K_m = 0.030 ± 0.012 mM and a Hill coefficient of 2.42 ± 0.17. Assays were performed in a buffer containing 200 mM 3,3-dimethylglutaric acid, pH 6.9 for 5 minutes at 295 K.

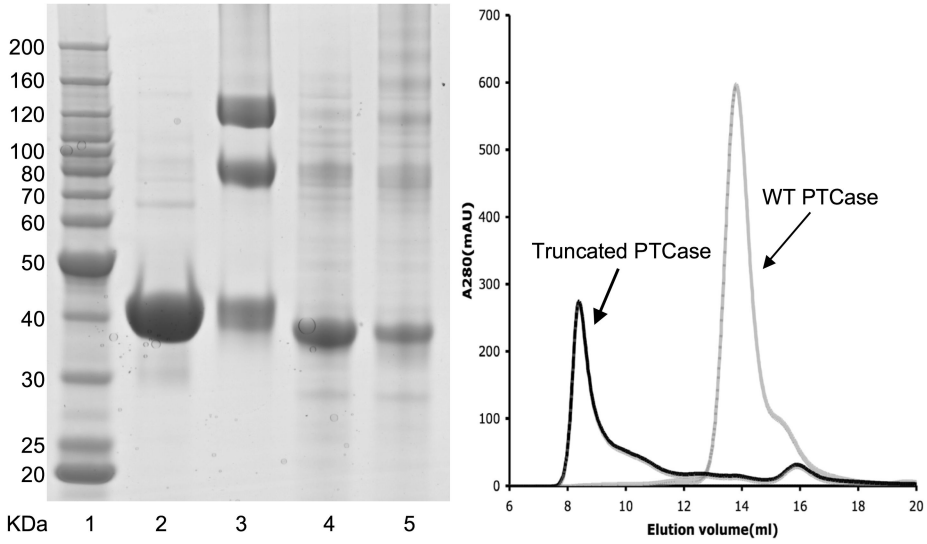

Figure 3.

Oligomeric structure of wild-type and truncated efPTCase in solution. *A*. Cross-linking of recombinant efPTCase and truncated efPTCase proteins with dimethyl suberimidate. efPTCase and truncated efPTCase (0.15 μg) were incubated with dimethyl suberimidate (0.25 μg) in 50 μl solution containing 200 mM triethanolamine, pH 8.25 overnight at 277 K. Lanes 1, protein size markers; 2, efPTCase without cross-linking reagent; 3, efPTCase with cross-linking reagent; 4, truncated efPTCase without cross-linking reagent; 5, truncated efPTCase with cross-linking reagent. *B*. Analytical gel chromatography of wild-type and truncated efPTCase. The elution profiles of wild-type and truncated efPTCase are shown in gray and black, respectively.

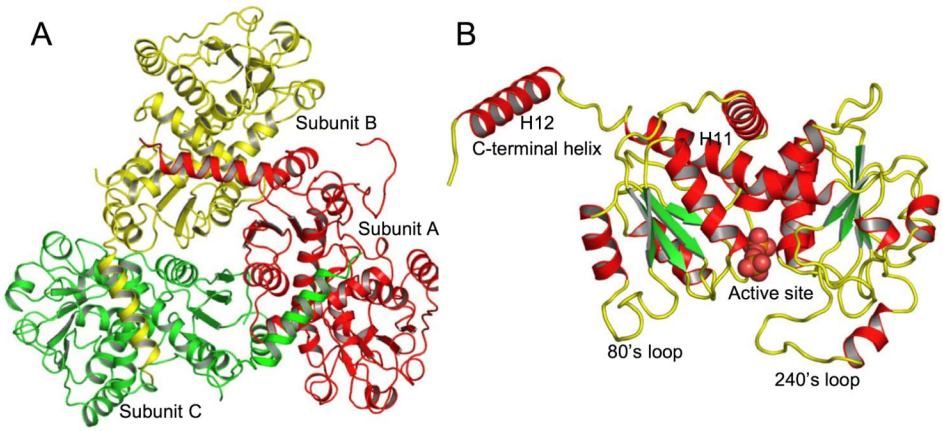

Figure 4.

Ribbon diagrams of the subunit and trimeric structures of efPTCase. A. Structure of molecular trimer of efPTCase. Different subunits are shown in different colors (subunit A, yellow; subunit B, red; subunit C, green). B. Structure of subunit B. The green arrows indicate the direction of strands in β sheets, α helices are in red, and β-sheets are in green. Bound sulfate groups are represented as a space-filling model.

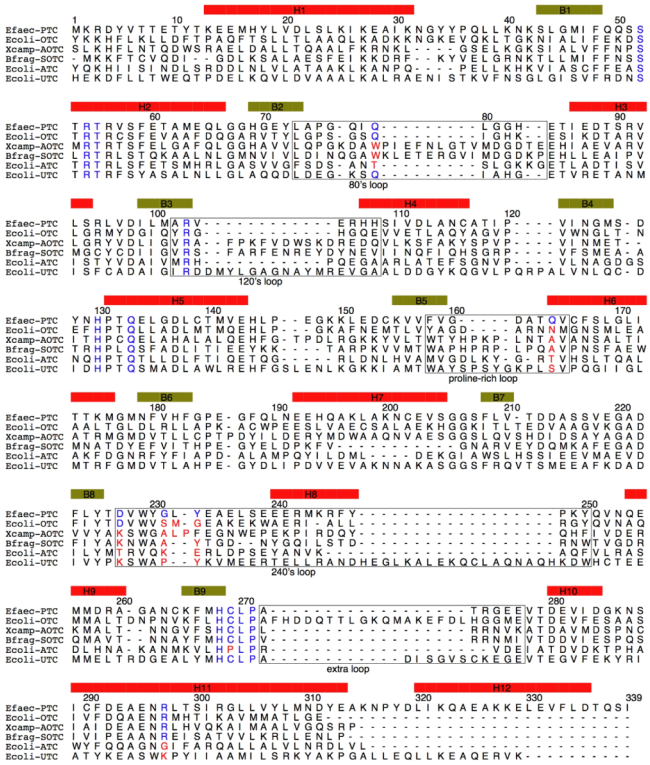

Figure 5.

Sequence alignment of efPTCase, *E. coli* OTCase, *X. campestris* AOTCase, *B. fragilis* SOTCase and *E. coli* UTCase. Sequences encoding secondary structure elements are indicated by boxes in yellow-green (β-strand) and red (α-helix). Amino acid residues that are proposed to bind ligands (CP or putrescine), are indicated in blue. Conserved equivalent residues in other carbamoyltransferases are shown in blue, non-conserved in red.

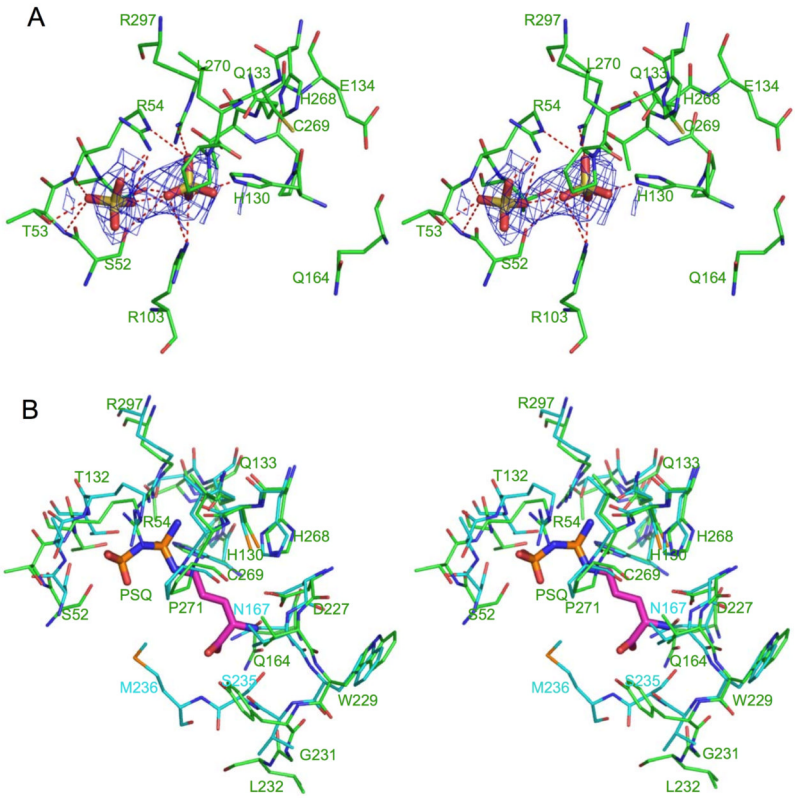

Figure 6.

Active site of subunit B. *A.* Stereo diagram of bound sulfate (shown as pink sticks) in the proposed active site. Electron density maps (*2Fo-Fc*) around bound sulfate are shown as blue cages, contoured at 1.0 σ. Hydrogen bonding interactions are shown as red dashed lines. *B.* Stereo diagram of the proposed active site of efPTCase (shown as light blue sticks) compared with ecOTCase (shown in green sticks, PDB accession number 1DUV). Bound N^{δ}-(N'-sulfodiaminophosphinyl)-L-ornithine (PSQ) is shown as pink sticks. The efPTCase residues are numbered in green. The ecOTCase residues which are different from equivalent efPTCase residues are numbered in light blue.

Table 1

Data Collection and Refinement Statistics

Data collection	
Space group	C2
Resolution range (Å)	50-3.2 (3.31-3.20)[a]
Unit-cell parameters	a = 273.86 Å
	b = 87.79 Å
	c = 241.30 Å
	β = 114.08°
Measurements	304,794
Unique reflections	85,439 (7,503)
Redundancy	3.6 (2.7)
Completeness (%)	98.5.5 (87.4)
$<I/\sigma(I)>$	10.0 (1.7)
R_{merg}(%)[b]	12.0 (46.8)
Refinement	
No. of protein atoms	31,977
No. of ligand atoms	185
RMSD of bond lengths (Å)	0.009
RMSD of bond angle (°)	1.3
R_{work} (%)[c]	19.0 (33.8)
R_{free}(%)[d]	23.4 (40.6)

[a] Figures in brackets apply to the highest-resolution shell.

[b] $R_{merg} = \sum h \sum i |I(h,i) - <I(h)>| / \sum h \sum i I(h,i)$, where $I(h,i)$ is the intensity of the ith observation of reflection h, and $<I(h)>$ is the average intensity of redundant measurements of reflection h.

[c] $R_{work} = \sum h |F_{obs} - F_{calc}| / \sum h F_{obs}$.

[d] $R_{free} = \sum h |F_{obs} - F_{calc}| / \sum h F_{obs}$ for 2.34% of the reserved reflections.